Soil Moisture Monitoring at the Field Scale Using Neutron Probe

Jayantha Kodikara[*!]
Associate Professor
Department of Civil Engineering
Faculty of Engineering, Building 60, Clayton campus
Monash University, VIC 3800, Australia
Phone: +61-3-9905 4963
Fax: +61-3-9905 4944
E-mail: jayantha.kodikara@monash.edu

Pathmanathan Rajeev[*]
Research Fellow
Department of Civil Engineering
Faculty of Engineering, Building 60, Clayton campus
Monash University, VIC 3800, Australia
Phone: +61-3-9905 1145
Fax: +61-3-9905 4944
E-mail: pathmanathan.rajeev@monash.edu

Derek Chan[*]
Postgraduate student
Department of Civil Engineering
Faculty of Engineering, Building 60, Clayton campus
Monash University, VIC 3800, Australia
Phone: +61-3-9905 5579
Fax: +61-3-9905 4944
E-mail: derek.chan@monash.edu

Chaminda Gallage[$]
Lecturer
School of Urban Development, Faculty Built Environment and Engineering
Queensland University of Technology (QUT - GP)
2 George St, Brisbane QLD 4001, Australia
Phone: +61-7-3138 1034
Fax: +61-7-3138 1170
E-mail: chaminda.gallage@qut.edu.au

[*] Monash University [$] Queensland University of Technology [!] Corresponding author

Soil Moisture Monitoring at the Field Scale Using Neutron Probe

J. Kodikara, P. Rajeev, D. Chan and C. Gallage

Abstract: Measurement of moisture variation in soils is required for geotechnical design and research since soil properties and behavior can vary as the moisture content changes. Neutron probe, which was developed more than 40 years ago, is commonly used to monitor the soil moisture variation in the field. This study reports a full-scale field monitoring of soil moisture using neutron moisture probe for a period of more than 2 years in Melbourne (Australia) region. On the basis of soil types available in Melbourne region, 23 sites were chosen for moisture monitoring down to a depth of 1500 mm. The field calibration method was used to develop correlations relating the volumetric water content and neutron counts. Observed results showed that the deepest "wetting front" during the wet season was limited to the top 800 mm to 1000 mm of soil whilst the top soil layer down to about 550 mm responded almost immediately to the rainfall events. At greater depths (550 to 800 mm and below 800 mm), the moisture variations were relatively low and displayed predominantly periodic fluctuations. This periodic nature was captured with Fourier analysis to develop a cyclic moisture model on the basis of an analytical solution of one-dimensional moisture flow equation for homogeneous soils. It is argued that the model developed can be used to predict the soil moisture variations as applicable to buried structures such as buried pipes.

Key words: Soil moisture content, neutron probe, field calibration, expansive soil, Fourier analysis, moisture diffusivity

1. INTRODUCTION

Large areas of the surficial soil formations in the world are covered by clay soils with high potential for swelling and shrinking, commonly referred to as expansive soils. Shrinking and swelling of expansive soil in response to water content or suction change is one of the commonest geotechnical causes of damage to light structures, road pavements and buried infrastructures (Jones and Holtz 1973; Krohn and Slossen 1980; Freeman *et al*. 1991). Richards *et al*. (1983) estimated that 20% of the surface soils of Australia can be classified as moderately to highly expansive. In fact, six out of eight of Australia's largest cities are significantly affected by expansive soils, which realise a significant proportion of their expansive potential (Fityus *at el*. 2004). Approximately half of the surface area in Victoria was covered by moderate to highly expansive soils; mostly derived from tertiary, quaternary and volcanic deposits (Mc Andrew 1965). Numerous light structures founded on expansive soils in Victoria suffered from ground movement due to heave or drying settlement in the clay beneath them. According to Archicentre Ltd. (2000), the western and north western suburbs in Melbourne showed significant foundation distress on average 50% of the houses. Gould et al. (2009) reported that the number of failures in the water and gas pipeline network have increased greatly in recent years across the world, especially in Australia. On the basis of field monitoring, Gallage et al. (2008) identified that the variation of soil moisture at the vicinity of the pipe leading to soil shrinkage/swelling and associated pipe deformation could develop pipe flexural stresses exceeding the strength of a corroded pipe. It follows then that the knowledge of seasonal soil moisture variation in expansive soil is important to determine the additional stresses and/or deformations that are imposes on the surficial structures.

In general, two different approaches have been reported in literature to calculate stresses and deformations on structures buried in or placed on expansive soil: (1) using suction as a governing variable (e.g., Fredlund and Vu, 2003; Masia et al., 2004); and (2) using moisture content as a governing variable (e.g., Fityus, 1999; Rajeev and Kodikara, 2011). Fredlund and Vu (2003) modelled the stress and deformation under the slab as a function of variation in matric suction, defined as the excess air pressure over the pore water pressure. Masia *et at*. (2004) undertook 3D numerical modelling of the expansive soil movement on the basis of soil suction profiles that developed beneath a structure. This numerical model was reported to be capable of generating continuous records of moisture variations and deformations over time on the basis of recorded climatic data and representative soil properties.

However, the long term monitoring of suction variation in filed is difficult and not reliable (Fityus, 1999; Gould *et al*, 2011). In contrast, the measurement of moisture content is relatively easy, hence a ground movement prediction method based on moisture content offers some advantages. A number of researchers have followed this approach including Fityus (1999) and Rajeev and Kodikara (2011).

The accurate measurement of soil moisture is straightforward by oven drying. However, this requires a soil sample to be retrieved and tested, commonly in the laboratory. For non-destructive measurement of soil moisture, indirect tests are used such as neutron probe, time or frequency domain reflectometry and radiometry in remote sensing. Each of these indirect methods offers merits and demerits for moisture measurement in the field. The neutron probe is suitable for measurements involving an estimate of moisture within the upper 1000 to 2000 mm of the soil and generally, a description of moisture variations over large study areas (Schmugge *et al*., 1980). The neutron probe has proved to provide satisfactory measurements in soil moisture investigations (Evett and Steiner, 1995). The time domain reflectometry (TDR) determines the apparent dielectric properties of the soil, which is empirically related to the volumetric soil moisture content. The method is relatively quick and independent of soil type and is suited to automatic measurements. Remote sensing using low band radiometry has demonstrated the ability to measure the spatial variation of soil moisture content in the near-surface soil layer under a variety of topographic and land cover conditions (Schmugge and Jackson, 1994; Walker *et al*., 2004). Although apparently less accurate for spot measurements, the advantage of this method is that it can be used to measure the soil moisture variation in very large areas in the order of km's. However, a major limitation is that it can only measure moisture content in the surficial layer of soil, typically within the top 10 to 15 centimetres.

In this study, the neutron probe is used to monitor the soil moisture variation in Melbourne region (in 23 sites) for 2 more than years down to a depth of 1500 mm. Most of the monitored sites (i.e., 17 out of 23 sites) are in the western and north-western suburbs in Melbourne, the surficial natural soils of which are classified as highly expansive soils. The neutron probe was calibrated to measure the volumetric water content using the neutron counts, the output of the neutron probe. The calibration was carried out using field calibration method. The moisture content was measured at depth intervals of 150, 250, 350, 450, 550, 800, 1200 and 1400 mm. On the basis of the soil types encountered, 23 sites were grouped into three main categories, namely basaltic clay, non basaltic clay and sandy soils. The variation of soil moisture over the measurement period was compared for each soil type.

Finally, a simplified cyclic moisture variation model based on the solution of the one-dimensional moisture flow equation for homogeneous soil was developed. The model was then used to back-figure the average moisture diffusivity of soil, arguably presenting a tool for the prediction of soil moisture fluctuation.

2. NEUTRON SCATTERING METHOD

The neutron method of measuring soil water content uses the principle of neutron thermalisation. Hydrogen nuclei have a marked property for scattering and slowing down neutrons. In presence of water molecules, high-energy neutrons emitted from a radioactive substance such as radium-beryllium or americium-beryllium slow down and change direction due to elastic collisions (i.e., thermalisation). The energy of the neutrons is reduced to about the thermal energy of colliding atoms of a substance at room temperature. Considering both energy transfer and scattering cross-section, it is evident that hydrogen, having a nucleus of about the same size and mass as the neutron, has a much greater thermalising effect than any other element. When both hydrogen and oxygen are considered, water has a marked effect on slowing or thermalising neutrons. Thermalised neutron density is easily measured with a detector, if the capture cross-section, except for that due to water, remains constant (i.e., chemical composition is constant), then the thermal neutron density may be calibrated against water concentration on a volume basis, i.e., giving the volumetric water content. Detailed information on the neutron scattering method and calibration method can be found in Rajeev *et al*. (2010).

A neutron probe consists essentially of two parts: (1) shield with probe; and (2) electronic counting system. The probe is a sealed metallic cylinder of 30 to 50 mm in diameter and 200 to 300 mm in length. It contains a radioactive source that emits fast neutrons, a slow neutron detector and a pre-amplifier. The signal of the pre-amplifier goes through a 5 to 20 m long cable to the electronic counting system. The schematic diagram of neutron probe is shown in Figure 1.

3. Site Selection and Characterization

The monitoring sites were selected on the basis of several selection criteria. First, the location of the site should be within the area of reactive soil reflected from the history of high pipe and light foundation failure rate. Second, surrounding areas of the sites need be clear of other utilities such as gas, power, telecommunications, storm water and sewer, and the nature strip needs to sufficiently wide to facilitate installation of the aluminium access tube with reasonable side clearance. Third, the ground surface needs to be reasonably flat to avoid potential of flooding and other adverse effects of a sloping ground. Last, the monitoring sites are to be located in a reasonably quiet area with low traffic flow, so that the vehicle carrying the neutron probe can be parked easily and the any disturbance to the public during monthly field measurements can be minimised.

As a desk-top study, the geological map of Melbourne (Rixon, 1973) was used to select potential suburbs with highly expansive soil (e.g., Older Volcanics and Newer Volcanics formations according to the local geology) and a considerable number of potential sites were identified using drive-by and walking surveys around these suburbs. A total of 50 sites were selected during the initial surveys and the corresponding authorities and local council were contacted prior to starting the work. Eventually, 23 sites were selected after considering the soil depth and the time required for monthly measurement. Figure 2 shows the location of all 23 monitoring sites around Melbourne. According to the Australian Standard of residential slab and footing design (AS2870, 1996), the change of suction depth in Melbourne area is approximately 1500 mm to 2300 mm, and from pervious field measurements

(Gallage et al. 2008; Gallage et al. 2009), it is found that the soil moisture content varies relatively less at a depth from 1700 to 2000 mm in Melbourne region in comparison to near surface soils. Therefore, the monitoring was undertaken up to the depth of 1500 mm.

Soil samples were collected from all the selected sites for classification. The soil tests were performed in accordance with the relevant Australian Standards. The particle size analysis (sieving and hydrometer), plastic limit, liquid limit and linear shrink test were performed. As mentioned above, 23 sites were grouped into three main categories depending on the soil type. Two representative sites per each category, which is six sites in total, were chosen to present the result and discussion due to the page limitation. Table 1 gives the soil classification data for the six sites chosen. Figure 3 shows the particle size distributions of soils at selected six sites.

4. FIELD INSTALLATION OF ACCESS TUBE

The measurement of moisture content using neutron probe requires an access tube to be installed permanently at each site. In this study, aluminium access tube is selected considering the factors such as susceptibility to corrosion, the need for mechanical strength, cost, the intended depth of installation and the need to obtain the maximum count rate. The access tubes used featured outer diameter of 50 mm and inner diameter of 46.8 mm, and were closed at the bottom by a tapered plug of the same material.

The hole in the ground for the access tube was prepared using a suitably sized soil auger. This method may be unsatisfactory in some cases, especially when the presence of stones can easily deflect the auger bit causing the hole to be non-uniform. The repeated movement of the auger up and down the hole when removing soil could enlarge the hole at the top, leaving room for water to run down the enlarged interface between the access tube and the ground. These difficulties were overcome by careful auguring and, in some cases, small amount of back filling to close the gap between the ground and the exterior of the aluminium tube.

The hand operated soil auger used to prepare the hole for access tube is shown in Figure 4. In most cases, the access tube provided a tight fit to augured hole and gentle use of the rammer was required to push it in. It was important to make sure that the tube bottom was well embedded in the undisturbed ground (or sitting on rock) in order to prevent the possibility of subsequent sinking of the tube that could lead to erroneous depth readings. The jutting out part of the access tube was cut at slightly below the ground level to conceal the tube from vandalism as well as in the case of grassed ground to allow mowing of the grass. A rubber bung was used to close the tube top, which was in turn was covered by a steel box (see Figure 5.b), which was eventually covered with soil or grass. Under favourable conditions, 3 to 4 access tubes were installed in a day.

5. CALIBRATION OF NEUTRON PROBE

Calibration of neutron probe involves correlating neutron counts with known volumetric water contents of the soil. Two approaches are commonly employed, namely laboratory drum calibration, and in situ or field calibration (Allen, 1993; Babalola, 1978). The laboratory calibration is made by packing a drum of suitable dimensions with soil at known moisture content, installing an access tube as used in the field and measuring the neutron probe counts. Then the process is repeated for a range of soil moisture contents. The radius of the drum must be larger than the radius of influence of the neutron probe to prevent neutron leakage. The soil used in laboratory calibrations should have the same elemental composition and bulk density as the soil in the field. However, it is usually difficult to reproduce in a drum the soil fabric found in situ (IAEA 1970).

Field calibrations are accomplished by correlating the probe readings in an access tube installed in the field, with the measured volumetric moisture contents of the soil along the tube (or possibly immediately adjacent to the tube). These comparisons have to be repeated at different times of the year, so as to sample the soil at different moisture contents, in such as case, further retrieving of soil samples adjacent to the access tube would be necessary. The volumetric moisture contents are usually estimated from gravimetric soil moisture content and soil density. However, it is often difficult to obtain representative undisturbed soil samples from heterogeneous soil profiles. In addition, the soil moisture content in the field may vary rapidly with depth, significantly complicating the interpretation of neutron readings. Detailed descriptions of the laboratory and field calibrations of neutron probe can be found in Greacen (1981) and IAEA (1970).

As stated above, the calibration of neutron probe consists of establishing a relation between probe output *cpm* (counts.min^{-1}) and soil volumetric water content θ [(cm^3 of H_2O).(cm^3 of bulk soil)$^{-1}$]. Theoretically, the same sample volume "exposed" to the neutrons (at a particular *cpm*) from the probe should be used to measure θ. However, this volume is not well defined (for instance, assumed to be a sphere of 100 to 400 mm diameter), and classical soil moisture measurement methods use samples significantly smaller. This disparity can be minimized by taking several soil samples for determining θ around the access tube near the position of the probe where *cpm* was obtained. In most cases, it is never guaranteed that both methods sampled the same volume of soil. The sampling problem becomes worse in heterogeneous, layered or stony soils.

Having obtained the best set of data possible, a calibration is made from pairs of data (*cpm* and θ). However, the use of a count ratio (n_{CR}) is preferred in place of *cpm* in order to avoid drifts, temperature and other effects on the electronics of the neutron probe. The count ratio n_{CR} is defined as:

$$n_{CR} = \frac{\text{count rate in soil}}{\text{count rate in standard}} = \frac{N}{N_S} = \frac{C.T^{-1}}{C_S.T^{-1}} \quad (1)$$

where C is number of counts measured in the soil during a period of time T (min), C_s number of counts measured in a standard material during a period of time T_s (min), N the count rate in the soil (*cpm*) and N_s the count rate in the standard material (*cpm*).

Further, the bulk density correction of the count ratio and water content data is carried out as proposed by Greacen and Schrale (1976). The corrected count ratio $n_{CR,C}$ and corrected water content θ_C, are determined from Eqs.(2) and (3) respectively:

$$n_{CR,C} = n_{CR}\sqrt{\frac{\rho_{bi}}{\rho_b}} \tag{2}$$

and

$$\theta_C = \theta\frac{\rho_{bi}}{\rho_b} \tag{3}$$

where ρ_{bi} = bulk density of soil at a given depth and ρ_b = average bulk density of the soil profile.

A least-squares linear regression of water contents on count ratios is developed using the corrected data. The calibration equation can be written as:

$$\theta_C = a + bn_{CR,C} \tag{4}$$

where *a* is intercept and *b* is calibration slope.

The intercept of a calibration curve varies from soil to soil and from probe to probe. It dose not need to pass through zero, since it is an extrapolated value, out of the calibration range. Although there is no strong theoretical meaning given to this intercept, it is considered to be related to the residual content of the soil.

The slope of the calibration also varies from soil to soil and from probe to probe. Being the derivative of the calibration line, it represents the sensitivity of the probe, namely the change in soil water content per unit change in the count ratio. Within certain limits, it can be said that the smaller is its value, the more sensitive the probe is. In other words, a small change in soil water content will show a significant change in count ratio, when the calibration slope is small.

Because of the processes of neutron interaction in the soil, geometry of the probe, type of neutron detector, electronics etc, each soil has a specific calibration line for a given neutron probe. Soil characteristics (mainly chemical composition and bulk density) also affect the calibration line. Therefore, for a specific soil, calibration lines are related to different soil bulk densities. In general, the calibration lines for different bulk densities of the same soil are parallel, having the same slope. For extremely layered soils, especially those with layers of different composition like some alluvial soils, the slopes differ for each layer (Greacen and Schrale, 1976).

In this study the field calibration method was adopted. Seven different sites around Melbourne region were selected for the field calibration of the neutron probe. A total of 62 disturbed samples of soil were collected from those fields at different depths. The gravimetric water content, w, was determined by weighing the samples before and after drying at 105°C over a 24h period. The bulk density (ρ_{bi}) was measured at each level of neutron probe readings in the laboratory. Table 2 gives the bulk density variations with depth for the seven sites.

The volumetric water content of each sample was calculated by the following formula:

$$\theta = \frac{\rho_{bi}}{\rho_w} w \tag{5}$$

The linear regression (calibration) lines were fitted for the seven sites using the corrected count ratio and calculated volumetric water content. Table 3 summarises the properties of the fitted calibration lines for seven sites (i.e., intercept, slope, and coefficient of determination).

The data collected from the site No 3 show a very poor linear correlation. It is suspected that the uncertain sampling protocol and the highly stratified soil profile resulted in the poor correlation between θ and *n*, on this occasion. To develop a general calibration equation for all 23 sites, the data collected from the six sites (except site No 3) were then combined for the regression analysis. The total number of data point used for the analysis is 53. Figure 6 shows the volumetric water content against corrected neutron count ratio together with the corresponding regression line for the combined data set. Figure 6 also shows the $\pm\sigma$ and $\pm 2\sigma$ lines from the mean.

The residuals (i.e., the difference between the measured values of water content and the corresponding values from the regression equation) were plotted as a function of the corrected count ratio to determine whether the data: (1) were homoscedastic such that the linear regression can be applied; and (2) were such that residuals did not have outliers greater than two standard deviations away from zero. On the basis of this analysis, two more data points, which yielded the residuals greater than two standard deviations away from zero, were removed.

Finally, after adjusting the data sets as described, a final least-squares regression was performed and the residuals were checked for homoscedasticity compliance again. Altogether 37 data points out of 51 points lie between $\pm$ one standard deviation from the regression line (i.e., more than 68% of the data lie within $\pm$ one standard deviation). So the data are approximately normally distributed about the regression line. Figure 7 shows the processed data and the corresponding regression line (Total of 51 data points). This regression line is considered as the overall calibration equation for volumetric water content with corrected neutron count ratio and is given as:

$$\theta = -0.050 + 0.318 n_{CR} \tag{6}$$

This equation is used to determine the volumetric water content variation in 23 sites using the periodic neutron probe measurements undertaken over more than 24 month period, as described in the following section.

6. Results and Discussion

The soil moisture changes with time due to local climate variations are given in Figure 8 to Figure 13 together with the rainfall data for the selected 6 sites. For each site, the corresponding rainfall data were obtained from the nearest monitoring station of the Department of Meteorology, Victoria. On the basis of the measured data and the magnitude of the moisture variation, each soil profile was divided into three primary layers. Figure 14 shows the moisture variation of basaltic clays with respect to the soil moisture content measured up to December 2011 The increase and decrease of moisture content in percentage was calculated with respect to the value at the beginning (i.e., June 2009). It is clear that the soil layer within top 550 mm was highly sensitive to rainfall as evident from the high moisture variation shown. At lower depths of 550 to 800 mm and below 800 mm, moisture variations were relatively low with wetting peaking around November 2009, and driest period occurring around February to March 2010. The moisture content in June 2010 was higher than that of the previous year.

Variations of soil moisture at non-basaltic clay sites are summarized in Figure 15. It is apparent that a significant peak and a relatively small peak of moisture content occur within the first year for the top 800 mm thick layer. For the layer below 800 mm depth, the peak of moisture content only occurred in November 2009, arguably as a result of the smoothing effect of moisture content in deeper soil. Figure 16 shows the variations of moisture content of Quaternary alluvial and tertiary sediments soils from the sites located at Eastern and Southern Melbourne. Since these soils are predominantly coarse grained soils, they are more sensitive to rainfall as moisture can seep relatively easily to deeper layers. The changes below 800mm depth (i.e., typical buried pipe depth) were greater than in other two categories of sites. However, the changes of soil volume (i.e., shrinking and swelling) due to moisture are expected to be less in these less reactive sediments.

7. MODELLING THE SOIL MOISTURE VARIATION

As indicated earlier, the knowledge of moisture variation in surficial soil is a key advantage in predicting the behaviour of structures that are either shallow buried or based on the ground. In addition, identifying current trends in moisture variation can help understand the likely future variation in moisture variations in short and long term, which can be due to perceived anthropological climate change effects. These models of moisture variation may then be used to quantify the effects of climate change on the surficial infrastructure. In the following section, a relatively simplified model attempting to capture the essential features of the moisture variation is presented. A detailed method of modelling climate/ground interaction in two of these sites were presented by Rajeev et al. (2012).

The annual variation of the monthly average soil moisture within the uniform soil at different depths is considered using the one-dimensional nonlinear diffusion equation:

$$\frac{\partial \theta}{\partial t} = \frac{\partial}{\partial z}\left\{ D(\theta)\frac{\partial \theta}{\partial z} \right\} \tag{7}$$

where θ is the volumetric soil moisture content at depth z at time t, and $D(\theta)$ is the soil moisture diffusivity.

In order to develop an analytical solution for the above non-linear equation, the following simplifying assumptions are made: (1) the soil surface (i.e., z = 0) is subjected to a harmonic sinusoidal moisture variation ignoring transient moisture variation due to rainfall events; (2) at infinite depth, the soil moisture is constant and is equal to the average soil moisture content; (3) a constant average moisture diffusivity is used throughout the soil profile and throughout the year. In general, the moisture diffusivity depends on the soil water content. However, experiments with certain undisturbed field soils and clays have shown that the assumption of a rapidly increasing moisture diffusivity is too limiting (Kutílek and Valentova, 1986). In fact, the diffusivity may increase only mildly with moisture content (Clothier and White, 1981) or it may even remain constant or decrease with increasing water-content specially for heavy clays (Kutílek, 1984; Kutílek, 1983). The detailed experimental and numerical study by Kutílek (1984) showed that assuming constant moisture diffusivity is a good working approximation for clay soils. Further, the observed data showed that moisture variation at greater depths are not significant. Therefore, the assumption 3 is reasonably valid for practical applications in clay soils. Thus, the solution for the Eq.(7) can be presented as in Eq.(8) on the basis of the solution for one-dimensional heat flow problem given by Hillel (1982) and Marshall and Holmes (1988):

$$\theta(z,t) = \theta_0 + \theta_S \, e^{-z/d} \sin\left(\omega t - \frac{z}{d} + C_0\right) \tag{8}$$

where $\theta(z,t)$ is the soil moisture, θ_0 is average soil moisture at z over a single period, θ_S is surface soil moisture amplitude, C_0 is a phase angle correction, and ω is the angular frequency of periodic soil moisture fluctuation (i.e., $\omega = 2\pi / T$) where T is the time period. The damping depth d, which is a constant characterizing the decrease in soil moisture amplitude with an increase in distance from the soil surface, is defined in terms of moisture diffusivity through

$$d = \sqrt{\left(\frac{2D}{\omega}\right)} \tag{9}$$

However, variable weather conditions are not true harmonic function as depicted by the sinusoidal boundary condition. Thus, the solution given in Eq. (8) may not be strictly valid for variable weather conditions. As Hurley and Wiltshire (1992) explained in relation to temperature variation within soil, the variations in weather boundary condition can be captured by using Fourier analysis. If we consider the linear diffusion equation (with constant *D*) as in Eq. (7), the resulting Fourier solution for the variable weather boundary condition can be expressed as:

$$\theta(z,t) = \theta_0 + \sum_{L=1}^{\infty} R_L(z) Sin\left(L\omega t + \Phi_L(z)\right) \tag{10}$$

where

$$R_L(z) = \theta_{SL}\, e^{\left(\frac{-z\sqrt{L}}{d}\right)} \tag{11}$$

and

$$\Phi_L(z) = \frac{-z\sqrt{L}}{d} + C_L \tag{12}$$

In this equation, general periodic soil moisture variation is represented by a combination of infinite number of harmonics defined by *L*. Fourier analysis allows the computation of the coefficients $R_L(z)$, $\Phi_L(z)$, and θ_0 on the basis of a set of soil moisture measurements at different depths and times as given below.

$$R_L(z) = \sqrt{a_L^2(z) + b_L^2(z)} \tag{13}$$

$$\tan \Phi_L(z) = \frac{a_L(z)}{b_L(z)} \tag{14}$$

where

$$a_L(z) = \frac{\omega}{\pi} \int_0^{2\pi/\omega} \theta(z,t)\cos(L\omega t)dt \quad L > 0 \tag{15}$$

and

$$b_L(z) = \frac{\omega}{\pi} \int_0^{2\pi/\omega} \theta(z,t)\sin(L\omega t)dt \quad L > 0 \tag{16}$$

In this manner, higher harmonics are used to describe the periodic variation in soil temperature at different depths. The observed soil moisture data for 12 months are used develop the moisture model for each site and $R_L(z)$ and $\Phi_L(z)$ are computed on the basis of respective data for each site.

For temperature variation within soil layer, Van Wijk (1966) and Carson (1963) have shown that the slope of $\ln(R_L(z))$ vs. z will provide an estimate of thermal diffusivity of soil. Using this approach and Eq. (11), the slope of $\ln(R_L(z))$ vs. $z\sqrt{L}$ was used to calculate the moisture diffusivity k and the damping depth d. Similarly, from Eq.(16), the slope of $\Phi_L(z)$ vs. $z\sqrt{L}$ can also be used to estimate k and d. The slopes were determined for all dominant harmonics, and in a truly uniform bare soil the values for each k and d should be identical.

Fourier analysis was carried out using the measured moisture data in 2010 for all six sites. Finally, a linear relationship for $\ln(R_L(z))$ vs. $z\sqrt{L}$ is developed only for the dominant harmonics (i.e., 1st five harmonics). Figure 17 shows the linear fit of $\ln(R_L(z))$ vs. $z\sqrt{L}$ for basaltic clay and non basaltic clay sites. The linear fits for basaltic clay sites show good agreement with higher coefficients of determination in comparison to the non basaltic clay sites for all the dominant harmonics. The analysis indicated that for sandy soil sites, a linear fit for $\ln(R_L(z))$ vs. $z\sqrt{L}$ is not suitable. Using the slope of the linear correlations, the moisture diffusivity of the soil is calculated and summarized in

Table 4. The calculated moisture diffusivity values are in the reasonable order of heavy and light clay (e.g., Mitchell, 1980; Staple, 1964; Van den Berg and Louters, 1988).

Figure 18 shows the model predicted moisture variation together with measured moisture data, at different depth for Avondale Heights. The measured data which were used to develop the model is marked. Figure 19 shows the comparison of predicted and measured moisture contents. The model predictions show very good agreement with the measured data at greater depths (i.e., below 550 mm) and the variation between the predicted and measured data increases at shallow depths (i.e., up to 450 mm). The moisture variation at shallower depths is directly effected by climate events. Further, the rainfall is relatively high in the monitoring period compared to previous years, thereby leading to moisture build up in the ground. The moisture prediction model may be improved using 4 to 5 year monitored data to calibrate the model parameters. This is because the typically observed cycle of moisture build up and depletion in Melbourne, Australia is about 4 to 5 years (Rajeev *et al*. 2012).

8. SUMMARY AND CONCLUSION

This work has been undertaken to study the soil moisture variation at different depths along the soil profile in 23 sites around Melbourne region, Victoria, Australia. The neutron scattering method was used to monitor the soil moisture variation on monthly basis. The neutron probe is calibrated to get the volumetric water content from the collected neutron counts. The paper presents the data collected for more than two years including the rainfall data, the soil classification data for six representative sites, and soil moisture model developed to predict future moisture variations.

The monitored moisture data show that the soil moisture variation at a particular site depends on the soil type and the local climate variations. The moisture variation within shallower soils (i.e., up to 450 mm depth) closely follows the local climatic events. The moisture variation within deeper soils mostly depends on the soil type. If the soil is predominantly sandy, the water can infiltrate easily and the influence of local climate is felt to deeper soils (i.e., up to 1000 mm depth). In contrast, the infiltration of water is substantially slow in clayey soils (especially in shrinking/swelling soils), and therefore, the moisture variation within deeper soils depends also on the evaporation rate at the ground surface.

Consequently, the moisture content changes within deeper soils can have a time lag of three to four months or more in comparison to shallower soil. The data also indicates that the soil moisture changes at the deeper soils are also cyclic in nature.

A simplified moisture model is developed using the one-directional moisture flow equation for homogeneous soil with constant moisture diffusivity. This moisture diffusivity could be considered as an apparent value representative of the field soil profile considered. The Fourier analysis was carried out incorporate variable climatic conditions at the ground/soil interface and to find the average moisture diffusivity applicable to the zone of ground analysed. The basaltic and non-basaltic clays show reasonable the linear fits for magnitude of Fourier coefficients with depth but sandy soils do not show acceptable linear trends of these coefficients. For clay soils, it seems possible to back calculate the average moisture diffusivity using moisture content data using the simplified analysis proposed. Further, the model developed to predict the moisture variation shows good agreement with the monitored data at greater depths in comparison to the shallower depths. The model developed can be used to predict the future possible moisture variation in clayey soils due to climate events and may be applied to predict the soil movements and swelling stress induced on buried and on ground structures.

REFERENCE

Allen, R. G. (1993). Error analysis of bulk density measurements for neutron moisture gage calibration. Proc. ASCE Nat. Conf. on Irrigation and Drainage Engineering. Park City, UT, New York, ASCE. Management of Irrigation and Drainage Systems, Integrated Perspectives: 1120–1127.

Archicentre Ltd (2000), Cracking in Brickwork, Archicentre Ltd., Melbourne.

Babalola, O. (1978). Field calibration and use of the neutron moisture meter on some Nigerian soils, Soil Science 126, pp. 118-124.

Carson, J. E. (1963). Analysis of soil and air temperatures by Fourier techniques: Jour. Geophy. Res., Vol. 68(8), pp. 2217-2232.

Clothier, B. E. and White, I. (1981). Measurement of sorptivity and soil water diffusivity in the field, Journal of Soil Science Society American, Vol. 45, pp. 241-245.

Evett, S. R. and Steiner, J. L. (1995). Precision of neutron scattering and capacitance type moisture gages based on field calibration. Journal of Soil Science Society American, Vol. 59, pp. 961–968.

Fityus, S. G. (1999). A soil moisture based method of estimating y_s. Australian Geomechanics, Vol. 34(3), pp. 15–23.

Fityus, S. G., Smith, D. W. and Allman, M.A. (2004). Expansive soil test site near Newcastle. Journal of Geotechnical and Geoenvironmental Engineering, Vol. 130, No. 7, pp. 686-695.

Fredlund, D. G. and Vu, H. Q. (2003). Numerical modelling of swelling and shrinking soils around slabs-on-ground, PTI conference, Huntington Beach, California.

Freeman, T. J., Burford, D., and Crilly, M. S. (1991). Seasonal foundation movements in London clay. Proceeding of 4th International Conference on Ground Movements and Structures, Cardiff, Vol 4, pp. 485-501.

Gallage, C., Gould, S., Chan, D. and Kodikara, J. (2008). Field measurement of the behaviour of an in-service water reticulation pipe buried in reactive soil (Altona North, VIC), Monash University, Research Report RR12.

Gallage, C., Chan, D., Gould, S. and Kodikara, J. (2009). Field measurement of the behaviour of an in-service gas reticulation pipe buried in reactive soil (Fawkner, VIC), Monash University, Research Report, RR13.

Gould, S., Boulaire, F. and Kodikara, J. (2009). Understanding how the Australian climate can affect pipe failure. Proceedings of OzWater 09. AWA, Melbourne, Australia.

Gould, S.J.F, Kodikara, J., Rajeev, P., Zhao, X.L. and Burn, S. (2011). A new mathematical equation for void Ratio-water content-net stress surface of expansive soils, Canadian Geotechnical Journal, Vol. 48(6), pp. 867-877.

Greacen, E. L. (1981). Soil water assessment by the neutron method, E.L. Greacen (editor). CSIRO, East Melbourne, Victoria, Australia. 140 pp.

Greacen, E. L. and Schrale, G. (1976). The effect of bulk density on neutron meter calibration, Australian Journal of Soil Research, Vol. 14, pp. 159-169.

Hillel, D. 1982. Introduction to soil physics. Academic Press, San Diego, CA.

Hurley, S. and Wiltshire, R. J. (1993). Computing thermal diffusivity from soil temperature measurements. Computers & Geosciences, Vol. 19(3), pp. 475-477.

IAEA. (1970). Neutron Moisture Gauges, International Atomic Energy Agency (IAEA), Vienna.

Jones, D.E J., and Holtz, W.G. (1973). Expansive Soils – The hidden Disaster. Civil Engineering-ASCE, Vol.43, pp. 43-49.

Krohn, J.P. and Slosson, J.E. (1980). Assessment of expansive soils in the United States. Proceedings of the 4th International Conference on Expansive Soils, Denver, CO, Snethen D (ed.), pp. 596–608..

Kutílek, M. (1983). Soil physical properties of saline and alkali soils, in International Symposium on Isotope and Radiation Techniques in Soil Physics and Irrigation Studies, IAEA-FAO, 179 190.

Kutílek, M. (1984). Some theoretical and practical aspects of infiltration in clays with D — constant. In: J. Bouma and P.A.C. Raats (Editors), Proc. of the ISSS Symp. on Water and Solute Movement in Heavy Clay Soils. ILRI Publ. 37, Wageningen, pp. 114-128.

Kutílek, M. and Valentova, J. (1986). Sorptivity approximations, Transport in Porous Media 1, 57-62.

Marshall, T. J. and Holmes, J. W. (1988). Soil Physics. 2nd ed. Cambridge Univ. Press, New York.

Masia, M. J., Totoev, Y. Z. And Kleeman, P. W. (2004). Modeling expansive soil movement beneath structures, Journal of Geotechnical and Geoenvironmental Engineering, Vol. 130(6), pp. 572-579.

Mc Andrew, J. (1965). The geological Map of Victoria in Geology of Australia ore deposits. 8th Commonwealth Mining & Metallurgical Congress, Australia & New Zealand, Melbourne, AusIMM, 1, McAndrew J., Marsden M.A.H.(eds), pp. 440-449.

Mitchell, P. W. (1980). The structural analysis of footings on expansive soil, 2nd edition, P.W. Mitchell and Kenneth. W. G. Smith & Associates Pty. Ltd.

Popescu, M. E. (1979). Engineering problems associated with expansive clays from Romania. Engineering Geology, 14(1), pp. 43–53.

Rajeev. P., Chan, D., Kodikara. J. (2010). Field Measurement of Soil Moisture Content Using Neutron Probe, Technical Report No RR 15, Department of Civil Engineering, Monash University, Australia.

Rajeev. P., Chan, D., Kodikara. J. (2012). Ground-atmosphere interaction modelling for long term prediction of soil moisture and temperature, Canadian Geotechnical Journal, (under review)

Rajeev, P. and Kodikara, J. (2011) Numerical Analysis of an Experimental Pipe Buried in Swelling Soil, Journal of Computers and Geotechnics, Vol. 38(7), pp. 897-904.

Richards, B. G., Peter, P., and Emerson, W. W. (19830). The effects of vegetation on the swelling and shrinking of soils in Australia. Geotechnique, Vol. 33, pp.127–139.

Rixon, C.H. (1973). Geological Map of Victoria, Geological Survey of Victoria, Melbourne, Australia.

Schmugge, T., and Jackson, T.J. (1994). Mapping surface soil moisture with microwave radiometers. Meteorol. Atmos. Phys., Vol. 54, pp. 213-223.

Schmugge, T. J., Jackson, T. J. and McKim, H. L. (1980). Survey of methods for soil moisture determination, Water Resouces Research, Vol. 16(16), pp. 961–979.

Standards Australia. (1996). AS2870 Residential slabs and footings, Sydney, Australia.

Staple, W.J. (1964). Moisture tension, diffusivity, and conductivity of a loam soil during wetting and drying, Canadian Journal of Soil Science, Vol. 45, pp. 78-86.

Van den Berg, J. A. and Louters, T. (1988). The variability of soil moisture diffusivity of loamy to silty soils on marl, determined by the hot air method. J. Hydrol., 97, pp. 235-250.

Van Wijk, W. R. and deVries, D. A. (1966). Periodic temperature variations in a homogeneous soil. In van Wijk, W. R. (ed.), Physics of Plant Environment. 2nd Ed. North Holland Publishing Co., Amsterdam, 102-143.

Walker, J. P., Willgoose, G. R. and Kalma, J. D. (2004). In situ measurement of soil moisture: a comparison of techniques, Journal of Hydrology, Vol. 293, pp. 85-99.

LIST OF FIGURE

LIST OF TABLE LIST

Table 5. Summary of the soil classification test results

Oakleigh South		**Doveton**	
Plastic limit	-	Plastic limit	26.9
Liquid limit	-	Liquid limit	60.5
Plasticity index	-	Plasticity index	33.6
Linear shrinkage	-	Linear shrinkage	11.4%
Soil group	SM	Soil group	CH
Geological formation	Quaternary alluvial and tertiary sediments, gravel, clay	Geological formation	Quaternary alluvial and tertiary sediments, gravel, clay
Bulleen		**Heidelberg West**	
Plastic limit	20.7	Plastic limit	20.8
Liquid limit	49.8	Liquid limit	61.3
Plasticity index	29.1	Plasticity index	40.5
Linear shrinkage	14.2%	Linear shrinkage	16.2%
Soil group	CI	Soil group	CH
Geological formation	Non-basaltic clay	Geological formation	Non-basaltic clay
Avondale Heights		**Deer Park**	
Plastic limit	26.4	Plastic limit	30.8
Liquid limit	87.2	Liquid limit	108.4
Plasticity index	60.6	Plasticity index	77.6
Linear shrinkage	22.8%	Linear shrinkage	25.6%
Soil group	CH	Soil group	CH
Geological formation	Basaltic clay	Geological formation	Basaltic clay

Table 6. Variation of soil bulk density with depth

Site. No	Depth (mm)									Average Bulk density (g/cm^3)
	150	250	350	450	550	800	1000	1200	1400	
	Bulk density (g/cm^3)									
1	1.56	1.45	1.45	1.59	1.71	1.48	1.62	2.05	2.18	**1.68**
2	1.56	1.45	1.93	2.12	1.98	2.01	1.97	2.07	2.01	**1.90**
3	1.95	2.00	1.92	2.13	1.97	1.98	1.88	2.06	2.11	**2.00**
4	1.94	1.94	1.94	1.94	1.94	2.01	2.01	2.12	2.10	**1.99**
5	0.87	1.53	2.18	2.00	2.10	2.09	2.07	2.11	-	**1.87**
6	1.96	2.05	2.04	2.02	1.81	2.20	1.95	1.94	2.20	**2.02**
7	1.74	1.56	1.82	1.76	1.69	1.76	1.77	1.75	1.59	**1.72**

Table 7. **Summary of Regression Analysis Results and Local Error Estimates**

Site. No	1	2	3	4	5	6	7
Number of data points	9	9	9	9	8	9	9
R^2	0.961	0.853	0.053	0.953	0.875	0.584	0.705
a	-0.052	-0.594	+0.258	-0.158	-0.093	+0.003	-0.056
b	0.260	0.600	0.113	0.430	0.372	0.304	0.379

Table 8. Moisture diffusivity of soil

Site	Moisture diffusivity (mm^2/s)					
	1st harmonics	2nd harmonics	3rd harmonics	4th harmonics	5th harmonics	Average
Avondale Heights	0.0049	0.0126	0.0258	0.0505	0.0156	0.0219
Deer Park	0.0417	0.0789	0.0140	0.0789	0.0789	0.0585
Bulleen	0.2020	0.1403	0.0505	0.1031	0.5611	0.2114
Heidelberg West	0.0197	0.5611	0.0351	0.5611	0.5611	0.3476

Figures

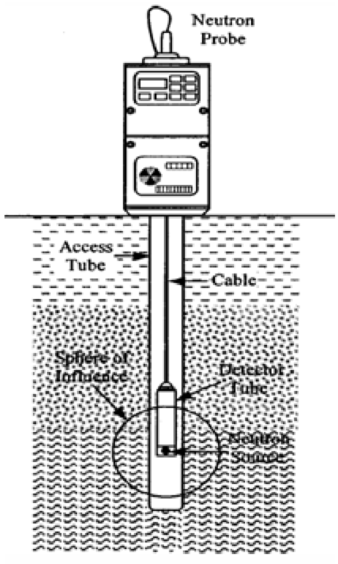

Figure 1. **Schematic of neutron probe**

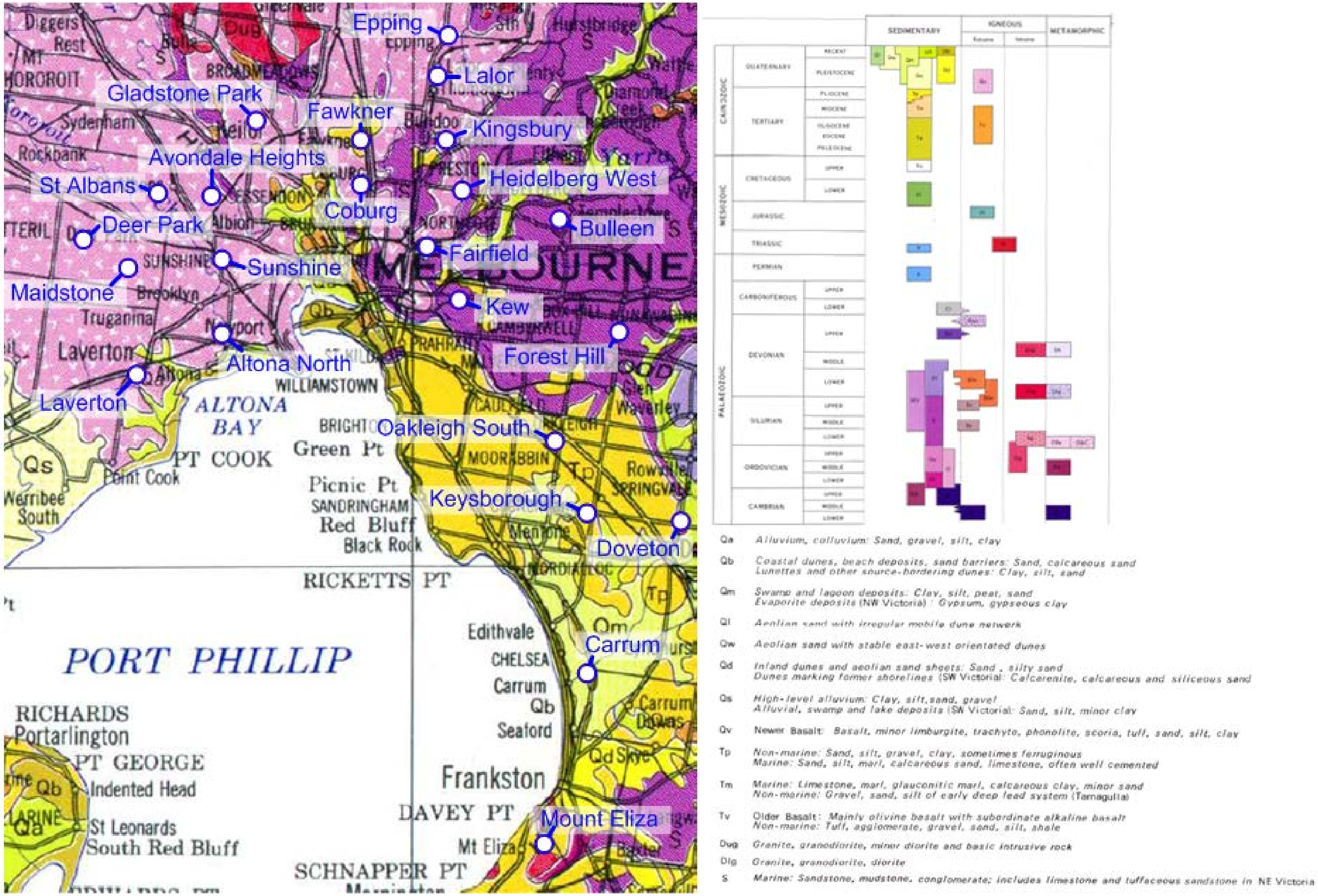

Figure 2. Location of the monitoring sites in Melbourne marked into geological map

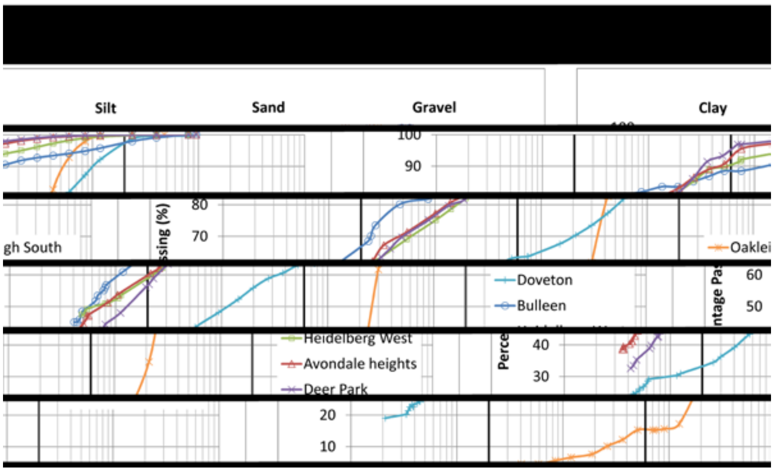

Figure 3. Particle size distribution of selected six sites

(a) (b)

Figure 4. (a) Schematic of hand soil auger, (b) making hole for access tube in the field

(a) (b)

Figure 5. (a) Pushing the access tube into the hole, (b) installed access tube protected by steel box

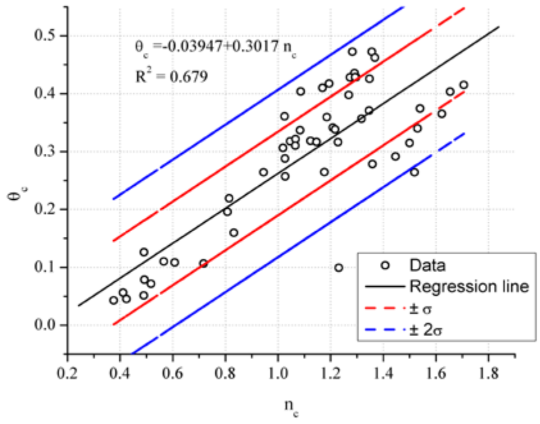

Figure 6. Combined data together with linear regression line

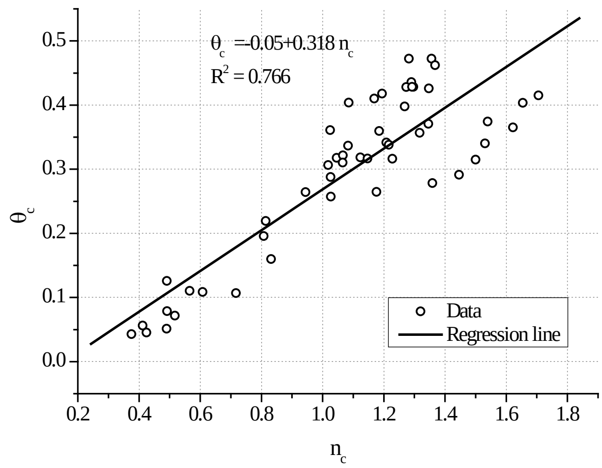

Figure 7. Cleared data points together with linear regression line

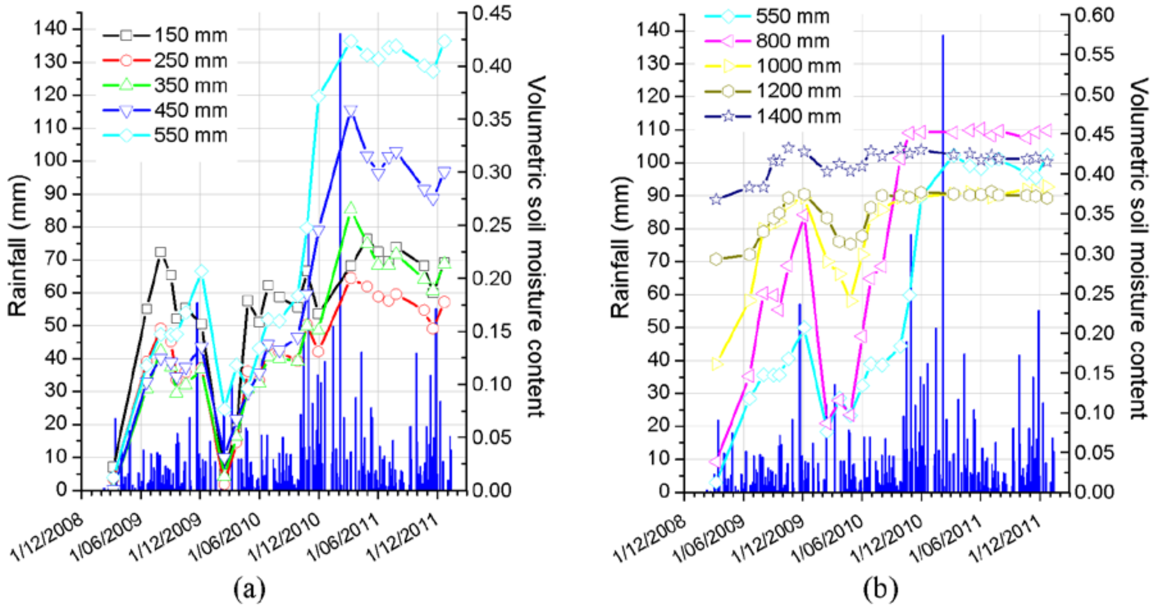

Figure 8. Oakleigh South soil moisture content data

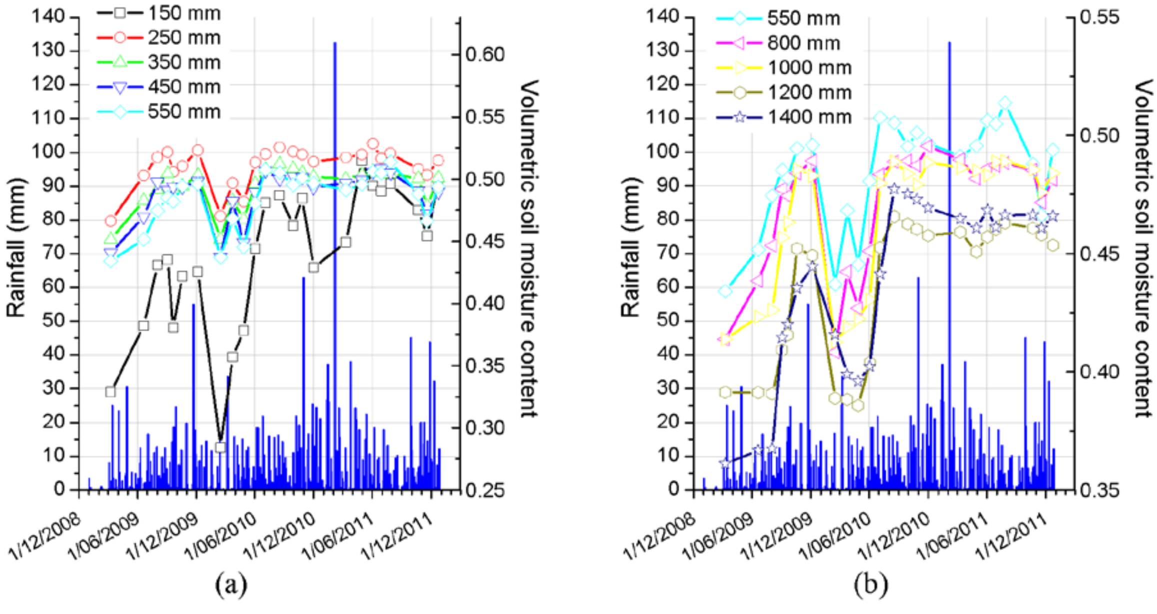

Figure 9. Doveton soil moisture variation

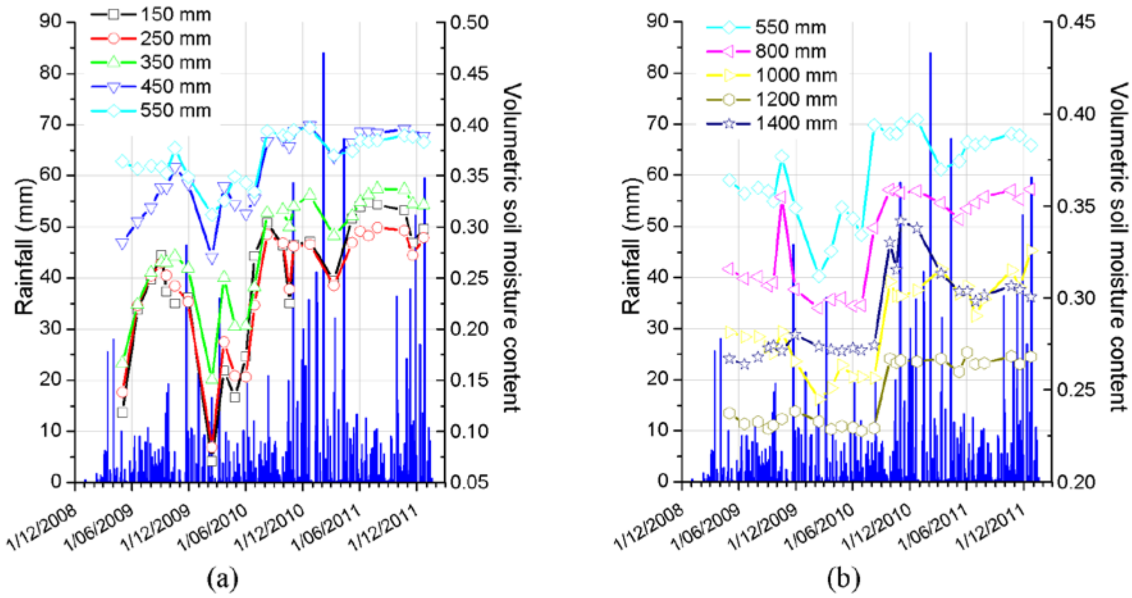

Figure 10. Bulleen soil moisture variation

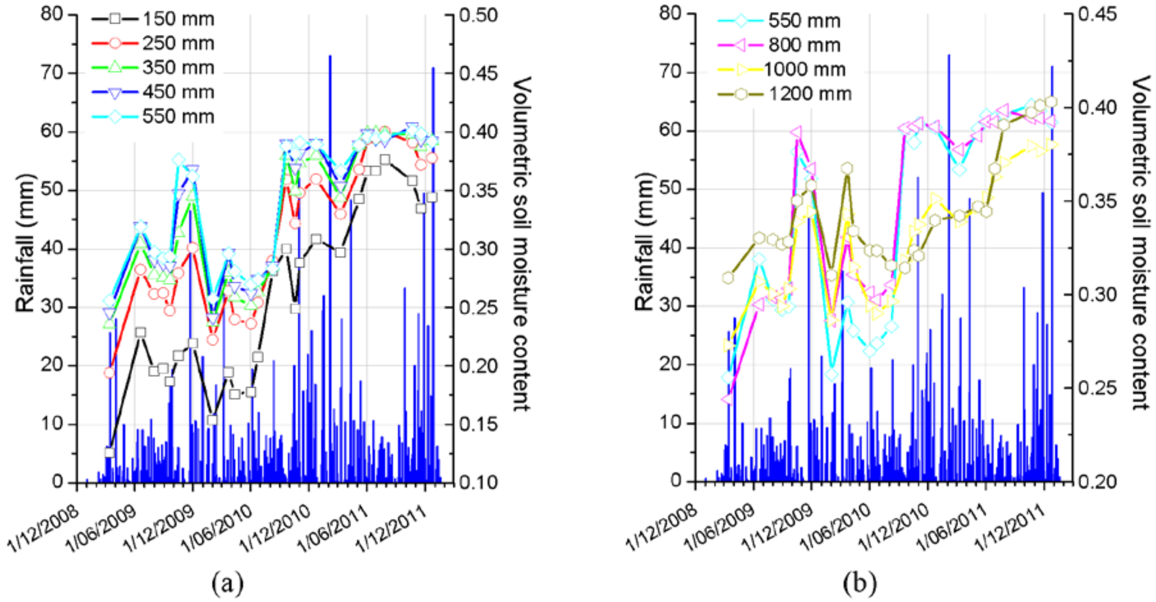

Figure 11. Heidelberg West soil moisture variation

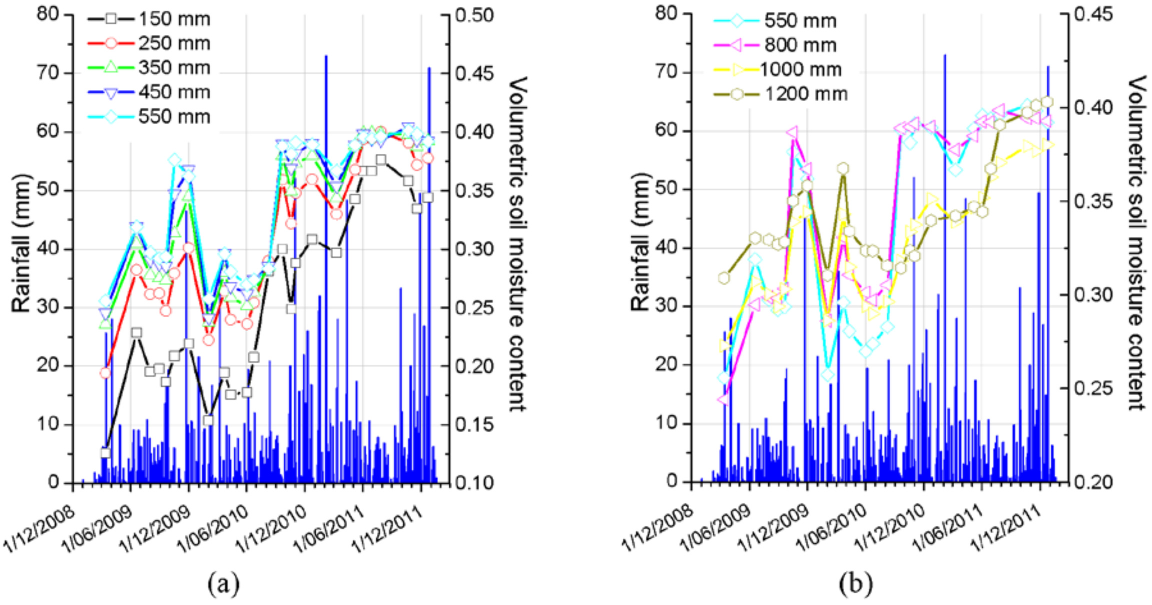

Figure 12. Avondale Heights soil moisture variation

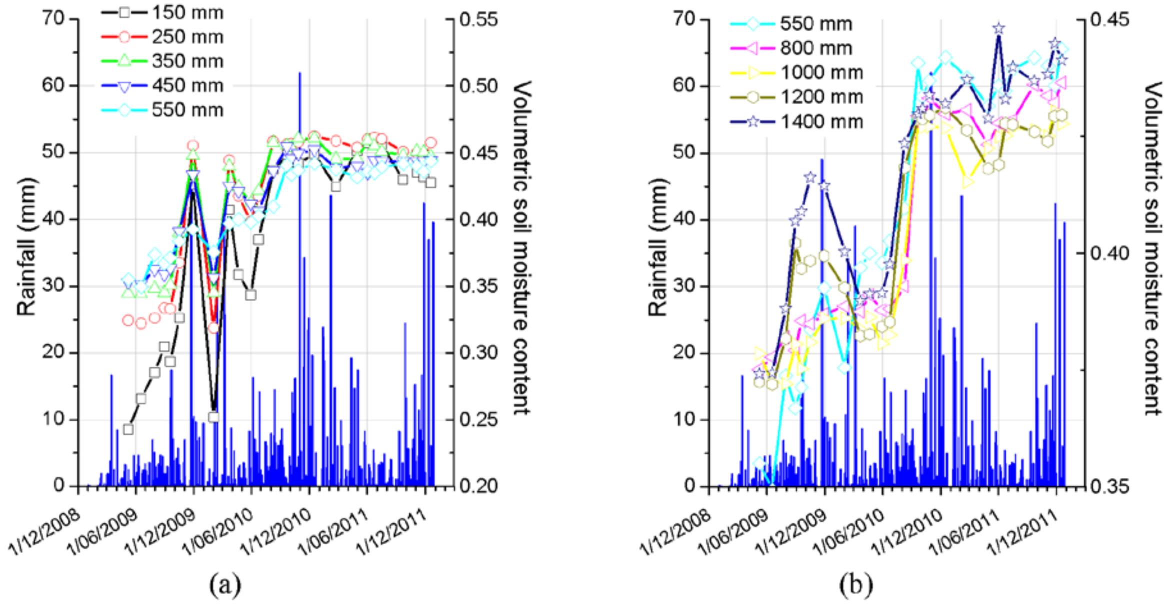

Figure 13. Deer Park soil moisture variation

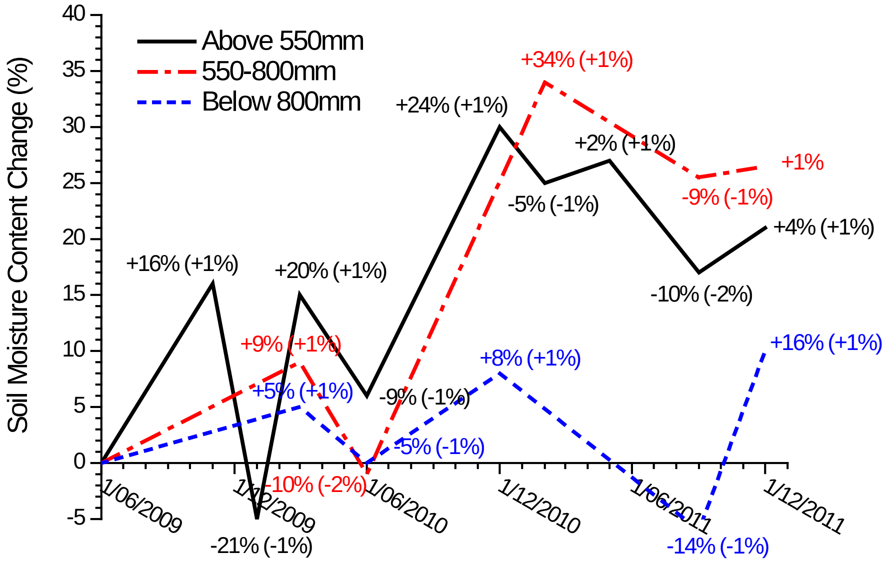

Figure 14. Soil moisture variation at each layer of Basaltic clays sites

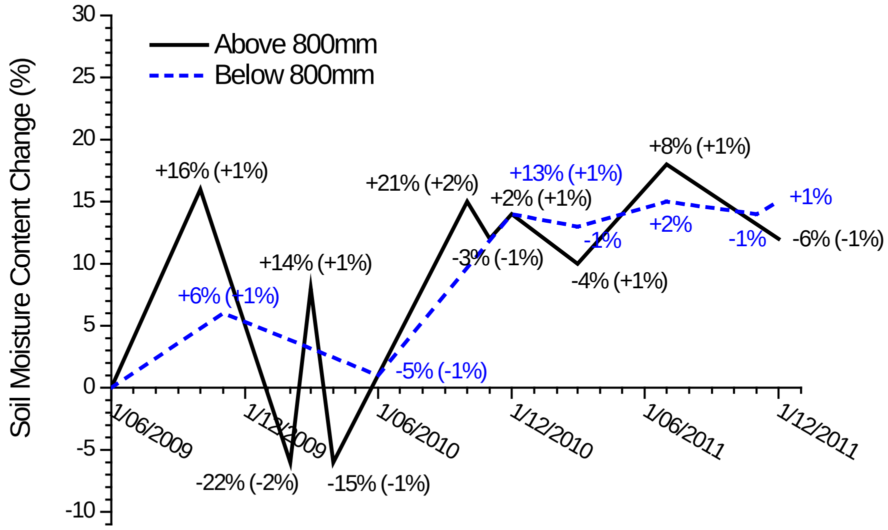

Figure 15. Soil moisture variation at each layer of Non-basaltic clays sites

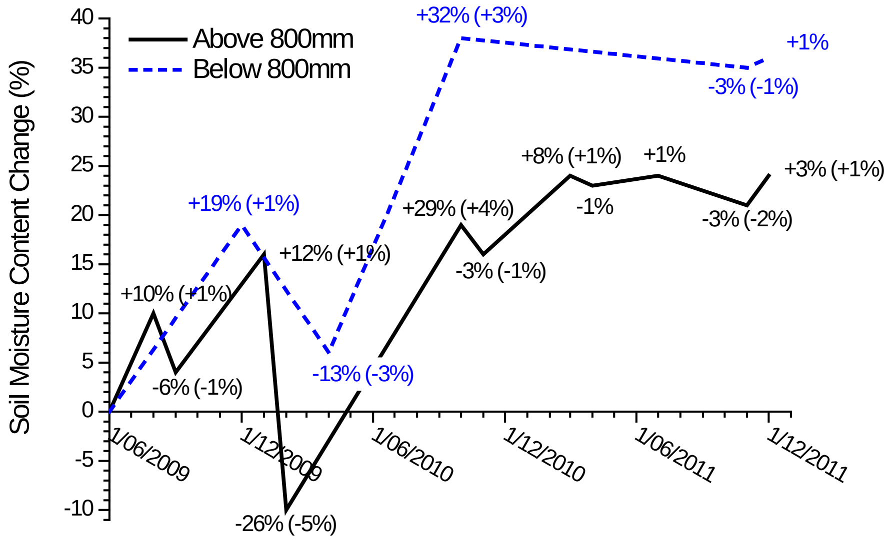

Figure 16. Soil moisture variation at each layer of Quaternary alluvials and tertiary sediments sites

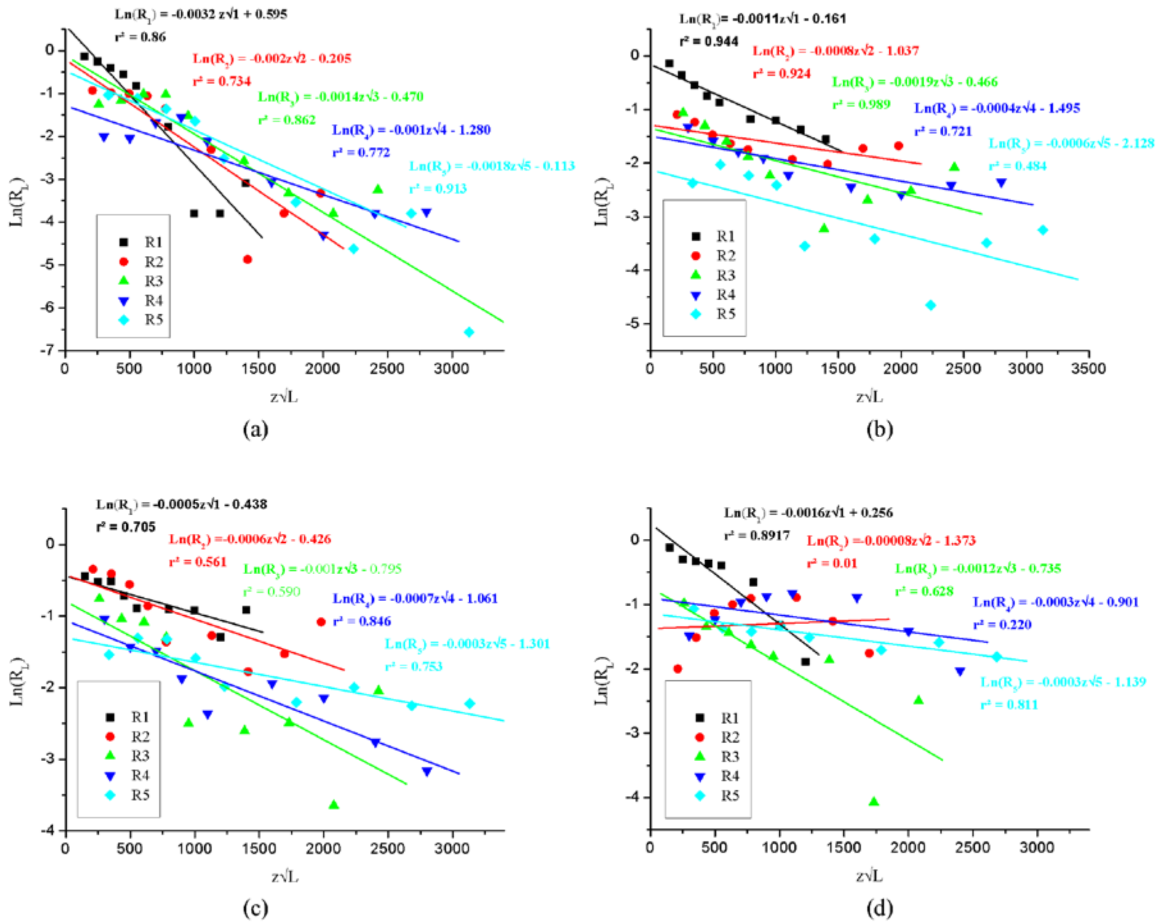

Figure 17. Linear fit of $R_L(z)$ vs. $z\sqrt{L}$: Basaltic clay sites (a) Avondale Heights, (b) Deer Park; and non basaltic clay site (c) Bulleen, (d) Heidelberg West

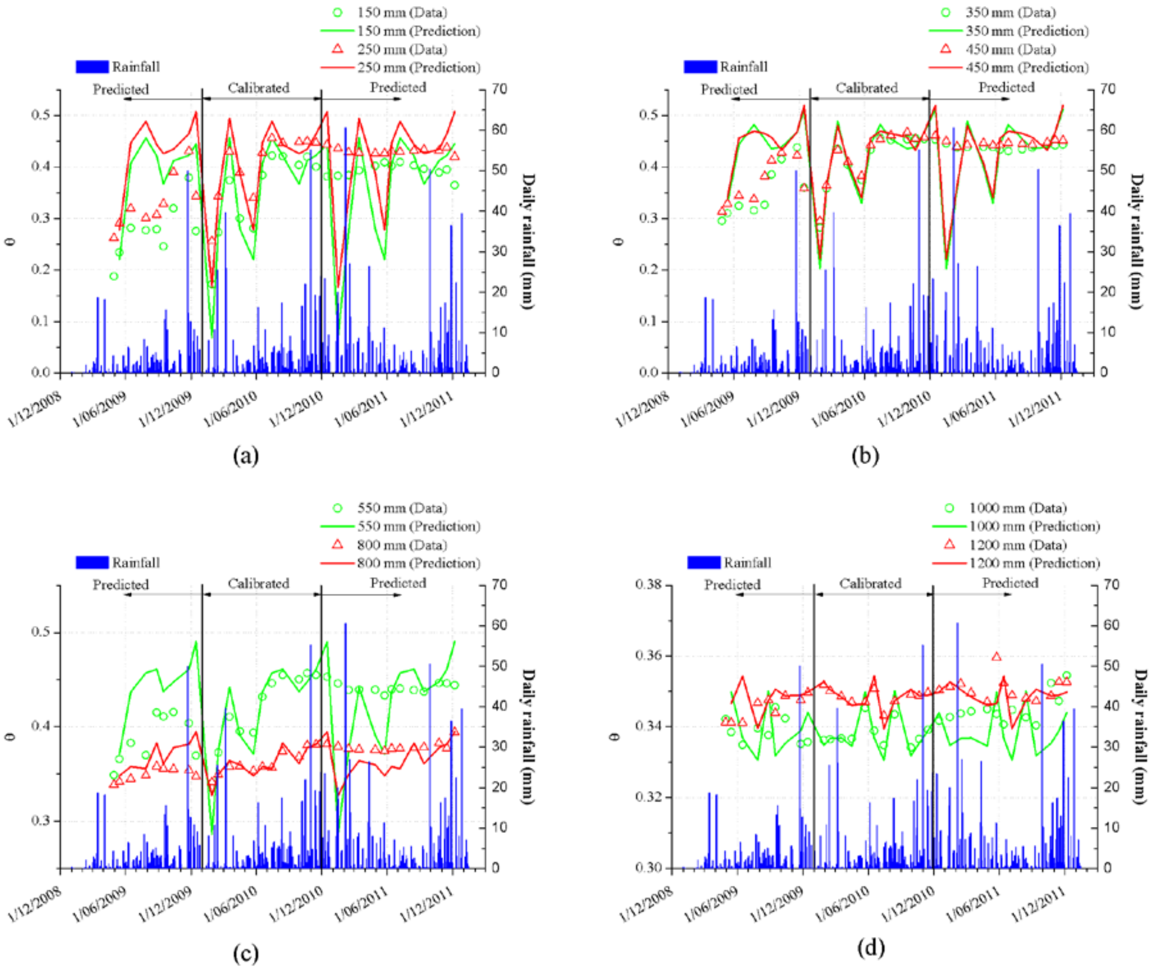

Figure 18. Neutron probe moisture data and the model prediction for Avondale Heights at different depth: (a) at 150 mm & 250 mm, (b) at 350 mm & 450 mm, (c) at 550 mm & 800 mm, (d) at 1000 mm & 1200 mm

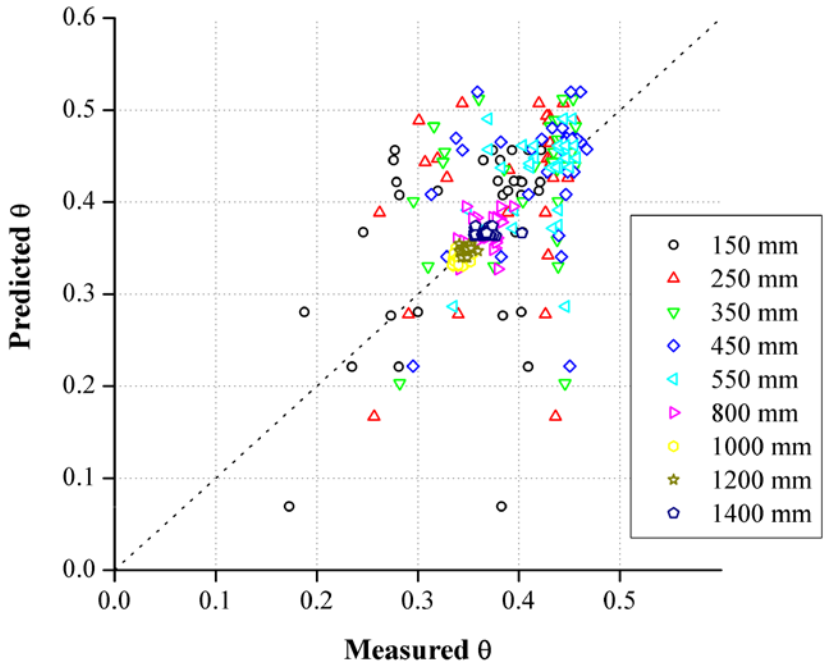

Figure 19. Comparison of measured and predicted moisture content